THE MARTIAN LOWER AND MIDDLE ATMOSPHERE AS OBSERVED BY THE MARS CLIMATE SOUNDER

D.J. McCleese, **J.T. Schofield**, **D.M. Kass, A. Kleinböhl**, **W.A. Abdou**, **R.W. Zurek**, **J.H. Shirley,** *Jet Propulsion Laboratory , California Institute of Technology, Pasadena, CA USA*, **S.B. Calcutt, P.G. J. Irwin, P.L. Read**, **F.W. Taylor**, **N. Teanby**, *University of Bristol, Bristol, UK*, **N.G. Heavens,** *Department of Earth and Atmospheric Sciences, Cornell University, Ithaca, NY, USA,* **M.I. Richardson**, *Ashima Research, Pasadena, CA*, **J.L. Bandfield**, *Department of Atmospheric Sciences, University of Washington, Seattle, Washington, USA,* **S.R. Lewis**, *Department of Physics and Astronomy, Open University, Milton Keynes, UK*, and **D.A. Paige**, *Department of Earth and Space Sciences, University of California, Los Angeles, CA, USA.*

Introduction:

The Mars Climate Sounder (MCS) has completed more than two Mars years of observations of the lower and middle atmosphere. MCS data extend the time and bridge the gap in the vertical coverage of the more than a decade-long, nearly continuous, climatology of Mars established by TES [*Smith et al., 2001 and Smith, 2004*], THEMIS [*Christensen, et al.,* 2003], PFS [*Formisano et al.,* 2005], aerobraking experiments [*Keating et al., 1998*], and SPICAM [*Forget et al, 2009*]. MCS is a nine-channel visible and infrared sounder that views the atmosphere in limb and near-nadir observing geometries with a vertical resolution of ~5 km [*McCleese et al.*, 2007]. The instrument is carried onboard the Mars Reconnaissance Orbiter [*Zurek and Smekar,* 2007]. First results of the MCS investigation were reported by *McCleese et al.*, [2008] showing the thermal structure of the atmosphere in northern summer and intense winter polar warming over the south pole.

Here we present and discuss global observations of zonal mean temperature, dust, and water ice from near the surface to above 80 km. The data were collected over a period of approximately 1.5 Mars years (MY) in MY 28 and 29. In this paper we focus on MY 29. *Kleinböhl et al.* [2009] describe the methodology for retrieving atmospheric properties from MCS measurements. Retrieved quantities presented in this paper result from an improved version of the retrieval scheme reported by *Kleinböhl et al.* [2009] and are available from the NASA Planetary Data System, Atmospheres Node.

Thermal Structure:

Figures 1 [*McCleese et al,* 2010, in press] shows the MCS retrieved nightside thermal structure of the atmosphere for MY 29 binned by Ls (5º), time of day (nightside is 21:00-9:00 LST), latitude (5º), and longitude (5.626º), and displayed at intervals of 45º in Ls. Zonal average temperatures in the pressure range 10^3 to 10^{-2} Pa are contoured every 5 K, and the CO_2 frost point is contoured in black. The extended vertical coverage of MCS, compared with earlier global data sets, reveals a nearly latitudinally symmetric middle atmosphere structure at northern spring equinox (Figure 1a), A warm region near the surface reaches from -45º to +45º latitudes. Middle-atmosphere polar warmings (0.1-10 Pa) extend from mid-latitudes to the poles in both hemispheres. An equator to pole 'Hadley' circulation is suggested. Only half a season later, Ls=45º (Figure 1b), the pattern is asymmetric with the warm lower atmosphere offset northward, extending from -30º to +60º. In the south, the polar warming is more confined vertically overlying an intensely cold middle atmosphere, near 140 k. In Figure 1c, the northern summer solstice, the thermal structure of the middle and lower atmosphere are little changed, MCS retrievals suggest that the warming has reached the north pole near the surface. In the second half of MY 29, Ls 180º to 270º, (Figures 1e-g) the lower atmosphere is significantly warmer, and the northern winter temperature minimum is less intense and confined to 75º to the pole, compared with -60º to the pole in southern winter.

Aerosol Distribution:

Figure 2 shows the zonal average dust density-scaled opacity (m^2kg^{-1}) for the nightside. We use density-scaled opacity to report MCS aerosol distribution because it is proportional to mass mixing ratio. The data are binned as in Figure 1. At the equinoxes (Figures 2a and 2e), dust penetrates higher into the middle atmosphere over the tropics with opacity falling rapidly poleward of $\pm$30º latitude. A clearing of dust develops at the northern summer solstice (Figure 2c) extending from -45º latitude to the south pole. Note that dust directly over the winter pole in this figures and in Figure 2g is more likely to be CO_2 ice than dust; CO_2 ice is not retrieved in our current retrieval scheme [*Kleinböhl et al.,* 2009]. Half a year later (Figures 2e-2g) the pattern of dust is quite different and the density-scaled opacity reaches its maximum value at northern winter solstice (Figure 2g). The clearing near the winter pole is much more tightly confined than it was in southern winter.

The vertical distribution of density-scaled dust opacity in the tropics in northern spring and summer (Figures 2a and 2c) has a maximum well above the surface, centered near 100 Pa (15-25 km altitude). In their paper *Heavens et al.* [2010, in preparation] assess the impact of this previously unobserved vertical distribution of dust on the radiative forcing of atmospheric circulation.

The seasonal evolution of water ice cloud is shown in Figures 3 and 4, nightside (21:00-9:00 LST) and dayside (9:00-21:00 LST) respectively, plotted as density-scaled ice opacity. Water ice clouds are present in the middle atmosphere at all times of the year, extending into the lower atmosphere at the equinoxes (Figures 3a and 4a). A broad, well delineated, tropical cloud belt is seen in northern spring and summer, while a less well organized cloud belt is apparent in southern spring and summer. The day–night variability of water ice clouds is apparent at all seasons, and especially in the tropics.

Summary

In this paper we present seasonal variations in zonal mean temperature, dust and water ice clouds of Mars. Resolving the vertical distributions of dust and water ice globally is a novel contribution from the MCS investigation. In particular, we show that in northern spring and summer the vertical distribution of dust does not exhibit the behavior inferred from previous studies (see for example *Conrath* [1975]), a result that is likely to be of interest to the Martian atmosphere modeling community.

Acknowledgements

We would like to thank Tina Pavlicek for her contributions to MCS instrument operations and Mark Apolinski for his work on processing the MCS data. Work at the Jet Propulsion Laboratory, California Institute of Technology, was performed under a contract with the National Aeronautics and Space Administration.

References

Christensen, P. R. *et al.* Mars: Mars Odyssey THEMIS (2003) Results *Science* 300, 2056;DOI: 10.1126/science.1080885

Conrath, B.J. (1975), Thermal structure of the Martian atmosphere during the dissipation of the dust storm of 1971, *Icarus*, *24*, 36-46.

Forget, F., F. Montmessin, J-L. Bertaux, F. Gonzalez-Galindo, S. Lebonnois, E. Quemerais, A. Reberac, E. Dimarellis, M.A. Lopez Valverde (2009), The density and temperatures of the upper martian atmosphere measured by stellar occultations with Mars Express SPICAM , *J. Geophys. Res.,* 114, E01004, doi:10.1029/2008JE003086.

Formisano, V. et al.: (2005) Calibration of the Planetary Fourier Spectrometer Short Wavelength Channel, *Planet. Space Sci.*, *53*, 975-991

Keating, G. M., et al. (1998) The Structure of the Upper Atmosphere of Mars: In Situ Accelerometer Measurements from Mars Global Surveyor, *Science,* 13, 279.5357.1672, doi: 10.1126/science.

Kleinböhl , A., J. T. Schofield, D. M. Kass, W. A. Abdou, C. R. Backus, B. Sen, J. H. Shirley, W. G. Lawson, M. I. Richardson, F. W. Taylor, N. A. Teanby, and D. J. McCleese (2009), Mars Climate Sounder limb profile retrieval of atmospheric temperature, pressure, dust, and water ice opacity, *J. Geophys. Res.*, *114*, E10006, doi: 10.1029/2009JE003358.

McCleese, D. J., J. T. Schofield, F. W. Taylor, S. B. Calcutt, M. C. Foote, D. M. Kass, C. B. Leovy, D. A. Paige, P. L. Read, and R. W. Zurek (2007), Mars Climate Sounder: An investigation of thermal and water vapor structure, dust and condensate distributions in the atmosphere, and energy balance of the polar regions, *J. Geophys. Res.*, *112*, E05S06, doi:10.1029/2006JE002790.

McCleese, D.J., J.T. Schofield, F.W. Taylor, W.A. Abdou, O. Aharonson, D. Banfield, S.B. Calcutt, N.G. Heavens, P.G.J. Irwin, D.M. Kass, A. Kleinböhl, W.G. Lawson, C.B. Leovy, S.R. Lewis, D.A. Paige, P.L. Read, M.I. Richardson, N. Teanby, and R.W. Zurek (2008), Intense Polar Temperature Inversion in the Middle Atmosphere on Mars, Nature Geosci., 1, 745-749, doi:10.1038/ngeo332.

McCleese, D.J., N.G. Heavens, J.T. Schofield, W.A. Abdou, J.L. Bandfield, S.B. Calcutt, P.G.J. Irwin, D.M. Kass, A. Kleinboehl, C.B. Leovy, S.R. Lewis, D.A. Paige, P.L. Read, M.I. Richardson, J.H. Shirley, F.W. Taylor, N. Teanby, and R.W. Zurek (2010), The Structure and Dynamics of the Martian Lower and Middle Atmosphere as Observed by the Mars Climate Sounder: 1. Seasonal variations in zonal mean temperature, dust and water ice aerosols, *J. Geophys. Res.,* in press, doi: 10.1029/2010JE003677.

Smith, M.D., J.C. Pearl, B.J. Conrath, and P.R. Christensen (2001). Thermal Emission Spectrometer results: Mars atmospheric thermal structure and aerosol distribution, *J. Geophys. Res.*, 106, 23,929-23,945.

Smith M.D. (2004), Interannual variability in TES atmospheric observations of Mars during 1999–2003. *Icarus* 167:148–65.

Zurek, R. W., and S. E. Smrekar (2007), An overview of the Mars Reconnaissance Orbiter (MRO) science mission, *J. Geophys. Res.*, *112*, E05S01, doi:10.1029/2006JE002701.

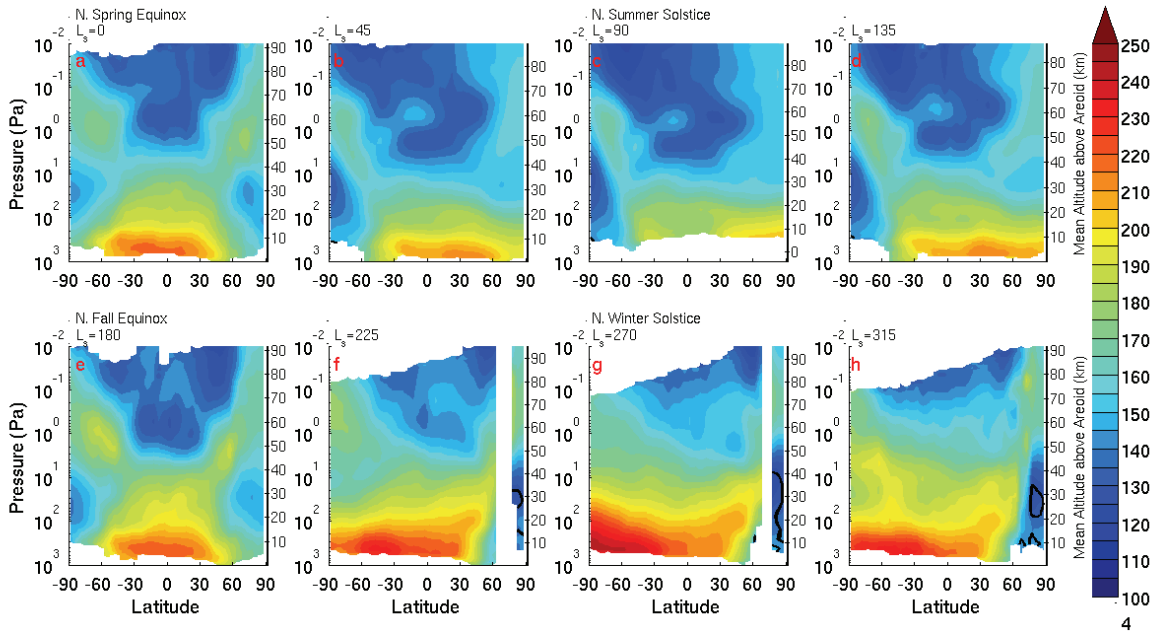

Figure 1: Zonal average temperature (K), nightside, MY 29 in bins of Ls. Contours are every 5 K.

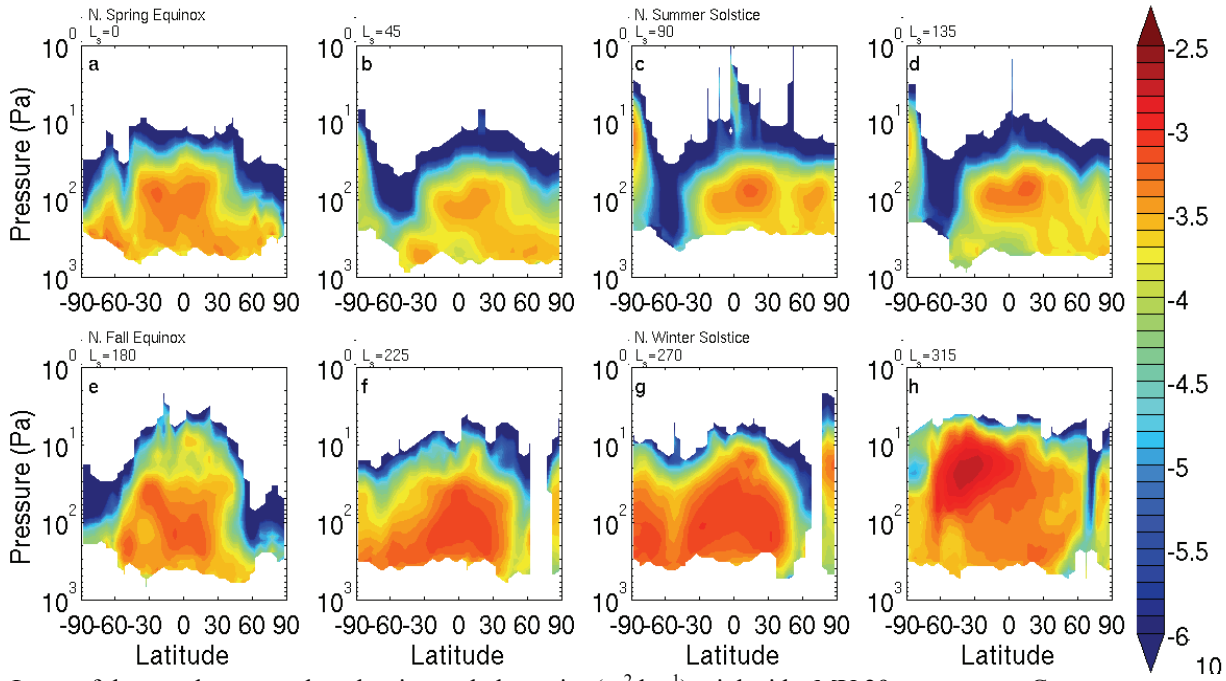

Figure 2: Log_{10} of the zonal average dust density-scaled opacity (m^2 kg^{-1}), nightside, MY 29 in bins of Ls. Contours are shown every 0.1 log units (the pressure scale is between 1000 and 1 Pa) [*McCleese et al,* 2010, in press].

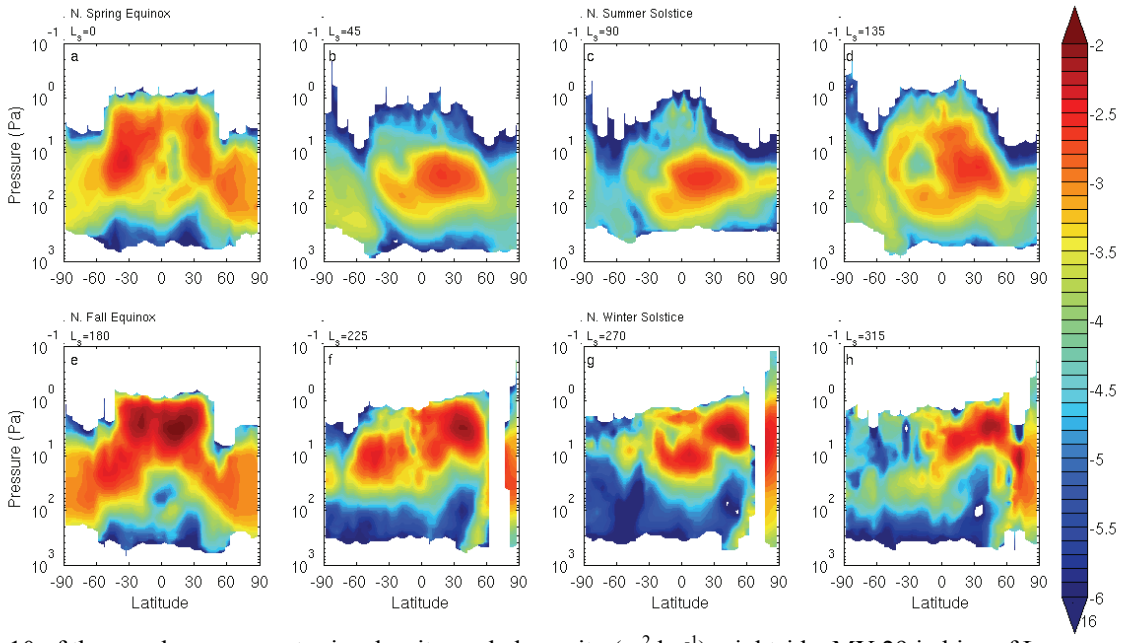

Figure 3: Log10 of the zonal average water ice density-scaled opacity (m^2 kg^{-1}), nightside, MY 29 in bins of Ls. Contours are shown every 0.1 log units (the pressure scale is between 1000 and 0.1 Pa) [*McCleese et al,* 2010, in press].

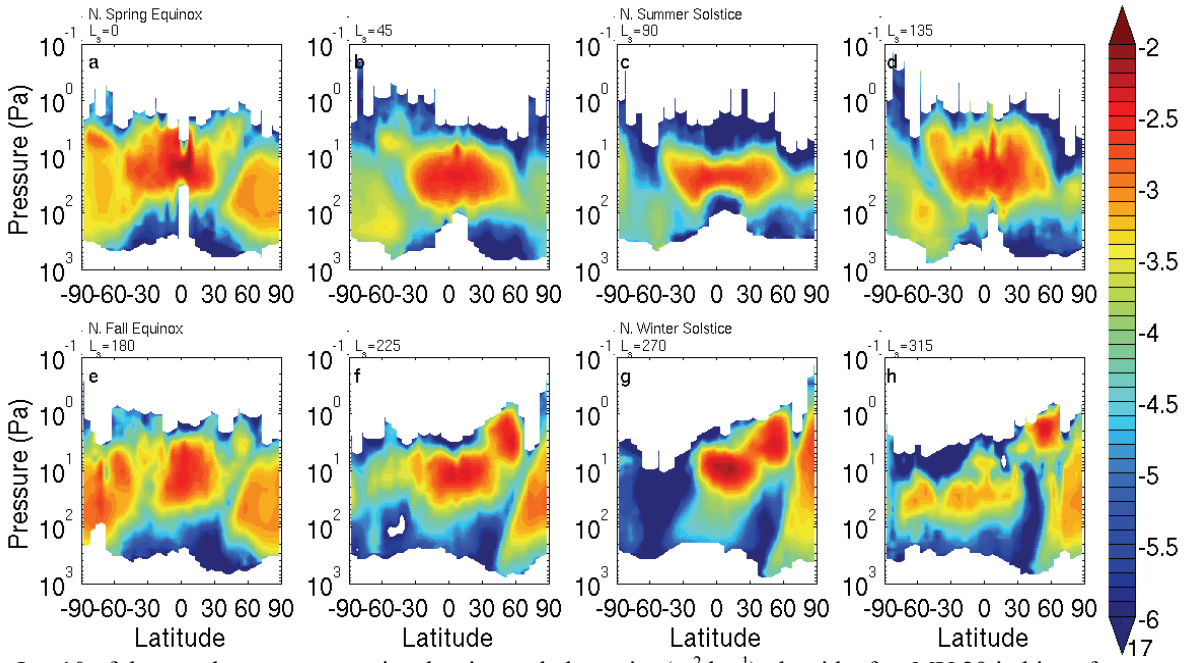

Figure 4: Log10 of the zonal average water ice density-scaled opacity (m^2 kg^{-1}), dayside, for: MY 29 in bins of Ls [*McCleese et al,* 2010, in press].